Double-hydrophilic block copolymer as an effective and green scale inhibitor in industrial recycling water systems

Guangqing Liu, Mengwei Xue, Qinpu Liu and Yuming Zhou

ABSTRACT

In an attempt to control $CaCO_3$ deposits in industrial recycling water systems, the performance of acrylic acid (AA)–allylpolyethoxy carboxylate (APEL) copolymer as an economical and environmentally friendly inhibitor have been investigated by static experiments, scanning electron microscopy (SEM), X-ray diffraction (XRD), and thermogravimetric analysis (TGA). The experimental results revealed that AA–APEL (acrylic acid–allylpolyethoxy carboxylate copolymer) achieved the maximum scaling inhibition efficiency of 99.1%. The results of SEM and XRD studies revealed that both the morphology and aggregation of calcium carbonate crystals had been changed, when the inhibitor was added. Moreover, the results of TGA further confirmed the scaling mechanism of the copolymer.

Key words | double-hydrophilic block copolymer, industrial recycling water, non-phosphorus, scale inhibitor, surface morphology

Guangqing Liu (corresponding author)
Mengwei Xue
Qinpu Liu
School of Environmental Science,
Nanjing Xiaozhuang University,
Nanjing 211171,
China
E-mail: *0539liuguangqing@163.com*

Guangqing Liu
Yuming Zhou
School of Chemistry and Chemical Engineering,
Southeast University,
Nanjing 211189,
China

INTRODUCTION

For environmental and economic reasons, a greater number of cycles for industrial water should be used. However, this cannot be realized without development of scale control methods (Ling *et al.* 2012; Wang *et al.* 2014; Al-Hamzah & Fellows 2015; Liu *et al.* 2016). The potential of mineral precipitation continues to be by far the most costly design and operating problem in recycling water systems (Al Nasser *et al.* 2011; Zhang *et al.* 2016). Commonly, mineral precipitation consists of calcium scales, zinc scales, magnesium hydroxide, ferric hydroxide, barium sulfate, etc., among which calcium carbonate scales are considered most frequent in cooling water systems (Alimi *et al.* 2006; Hasson *et al.* 2011; Wang *et al.* 2016).

The most common and effective method of scale control is the use of chemical additives as scale inhibitors that retard or prevent scale formation even in very small concentrations (Zhang *et al.* 2016). At present, amino trimethylene phosphonic acid (ATMP) and 2-phosphonobutane-1,2,4-tricarboxylic acid (PBTCA) are well-known scale inhibitors in cooling water systems. Although the nitrogen- and phosphorus-containing scale inhibitors are highly efficient, their use is limited because these compounds are nutrients for algae, which has the potential to ruin the environment (Koelmans *et al.* 2001). Under the pressure of worsening global ecological and environmental problems, the concept of 'Green Chemistry' was proposed and green scale inhibitors became a focus of water treatment technology.

In recent years, no-phosphorus copolymers have attracted great interest, both in industry and in academia. Polycarboxylates such as polyacrylic acid (PAA), polymaleic acid (PMA) and polyepoxysuccinic acid (PESA) are environmentally benign inhibitors. But they will react with calcium ions to form insoluble calcium–polymer salts, so they have a low calcium tolerance (Wang *et al.* 2010). Thus, novel scale inhibitors should be further developed to offer a high calcium tolerance and should be environmentally acceptable water additives.

In the present work, a polyether-type scale inhibitor, double hydrophilic block copolymer acrylic acid–allylpolyethoxy carboxylate (AA–APEL) was synthesized. In

doi: 10.2166/ws.2017.018

comparison with traditional scale inhibitors, AA–APEL derived from capped polyether is easily prepared with non-toxic, biodegradable, lower cost, reliable reproducibility and lower dosages, and has superior scale inhibitive performances. In addition, AA–APEL is an environmentally friendly scale inhibitor, only containing the three elements of carbon (C), hydrogen (H), and oxygen (O), and is free of phosphorus (P) and nitrogen (N).

EXPERIMENTAL SECTION

Materials and characterization

APEL was synthesized (Figure 1) from allyloxy polyethoxy ether (APEG) in our laboratory according to Fu *et al.* (2011). AA was analytically pure grade and was supplied by Zhongdong Chemical Reagent Co. (Nanjing, Jiangsu, China). Distilled water was used for all the studies.

Structures of APEG, APEL and AA–APEL were also explored with a Bruker NMR analyzer (AVANCE AV-500, Bruker, Switzerland) operating at 500 MHz. The X-ray diffraction (XRD) patterns of the $CaCO_3$ crystals were recorded on a Rigaku D/max 2400 X-ray powder diffractometer with Cu Kα($\lambda = 1.5406$) radiation (40 kV, 120 mA). Powder samples were mounted on a sample holder and scanned at a scanning speed of 2° min^{-1} between $2\theta = 20$–60°. The shape of the calcium carbonate scale was observed with a scanning electron microscope (S-3400N, Hitech, Japan). Thermogravimetric analysis (TGA) was performed on samples at temperatures ranging from 25 °C to 600 °C. Such signals were obtained at a heating rate of 20 °C/min in air using a Perkin-Elmer Derivatograph instrument.

Synthesis of AA–APEL

A five-neck round bottom flask, equipped with a thermometer and a magnetic stirrer, was charged with 100 mL distilled water and 0.1 mol APEL and heated to 65 °C with stirring under a nitrogen atmosphere. After that, 1.0 mol AA in 16 mL distilled water (the mole ratio of APEL and AA was 1:10) and the initiator solution (0.5 g ammonium persulfate in 15 mL distilled water) were added separately at constant flow rates over a period of 2.0 h. The reaction was then heated to 75 °C and maintained at this temperature for an additional 1.5 h, ultimately affording an aqueous copolymer solution containing approximately 30% solid. The synthesis of AA–APEL is given in Figure 2.

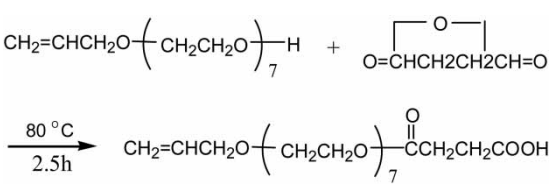

Figure 1 | Synthesis of APEL.

Precipitation conditions

All precipitation experiments were carried out in flask tests and the inhibitor dosages given below are on a dry-inhibitor basis. Tests of the inhibitor were carried out using supersaturated solutions of $CaCO_3$ at 60 °C. The solutions were prepared by dissolving in distilled water reagent grade $CaCl_2$ and $NaHCO_3$ (Zhongdong Chemical Reagent Co.). Each inhibition test was carried out in a flask of 500 mL immersed in a temperature-controlled bath for 10 h. Precipitation of $CaCO_3$ was monitored by analyzing aliquots of the filtered (0.22 μm) solution for Ca^{2+} ions using EDTA complexometry as specified in code GB/T 15452–2009. Inhibitor efficiency was calculated from the following equation:

$$\text{inhibition}(\%) = \frac{[Ca^{2+}]_{final} - [Ca^{2+}]_{blank}}{[Ca^{2+}]_{initial} - [Ca^{2+}]_{blank}}$$

where $[Ca^{2+}]_{final}$ is the concentration of Ca^{2+} ions in the filtrate in the presence of the inhibitor after calcium carbonate supersaturated solutions were heated for 10.0 h at 60 °C,

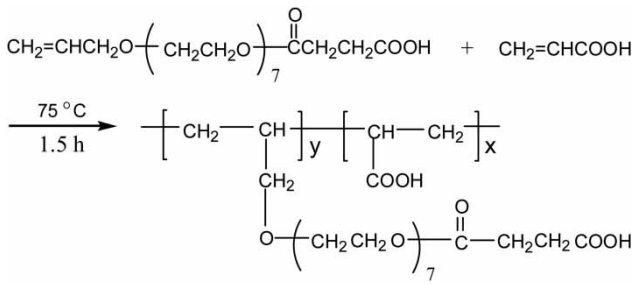

Figure 2 | Synthesis of AA–APEL.

$[Ca^{2+}]_{blank}$ is the concentration of Ca^{2+} ions in the filtrate in the absence of the inhibitor after calcium carbonate supersaturated solutions were heated for 10.0 h at 60 °C, and $[Ca^{2+}]_{initial}$ is the concentration of Ca^{2+} ions at the beginning of the experiment.

RESULTS AND DISCUSSION

Characterization of inhibitor

APEG ($(CD_3)_2SO$, δppm): 2.50 (solvent residual peak of $(CD_3)_2SO$), 3.00–3.80 ($-OCH_2CH_{2-}$, ether groups), 3.80–6.00 ($CH_2{\cdot}CH\text{-}CH_{2-}$, propenyl protons), 4.40–4.60 (−OH, active hydrogen in APEG) (Figure 3(a)).

APEL ($(CD_3)_2SO$, δppm): 2.25–2.55 ($-CH_2CH_{2-}$, protons in $-COCH_2CH_2COOH$), 2.50 (solvent residual peak of $(CD_3)_2SO$), 3.00–3.80 ($-OCH_2CH_{2-}$, ether groups), 3.80–4.10 and 5.00–6.00 ($CH_2{\cdot}CH\text{-}CH_{2-}$, propenyl protons) (Figure 3(b)).

The δ4.40–4.60 ppm (OH) active hydrogen in (a) disappeared completely and ($-CH_2CH_{2-}$) protons in $-COCH_2CH_2COOH$ appear obviously in δ2.25–2.55 ppm in (b). This proves that −OH in APEG has been entirely replaced by $-COCH_2CH_2COOH$.

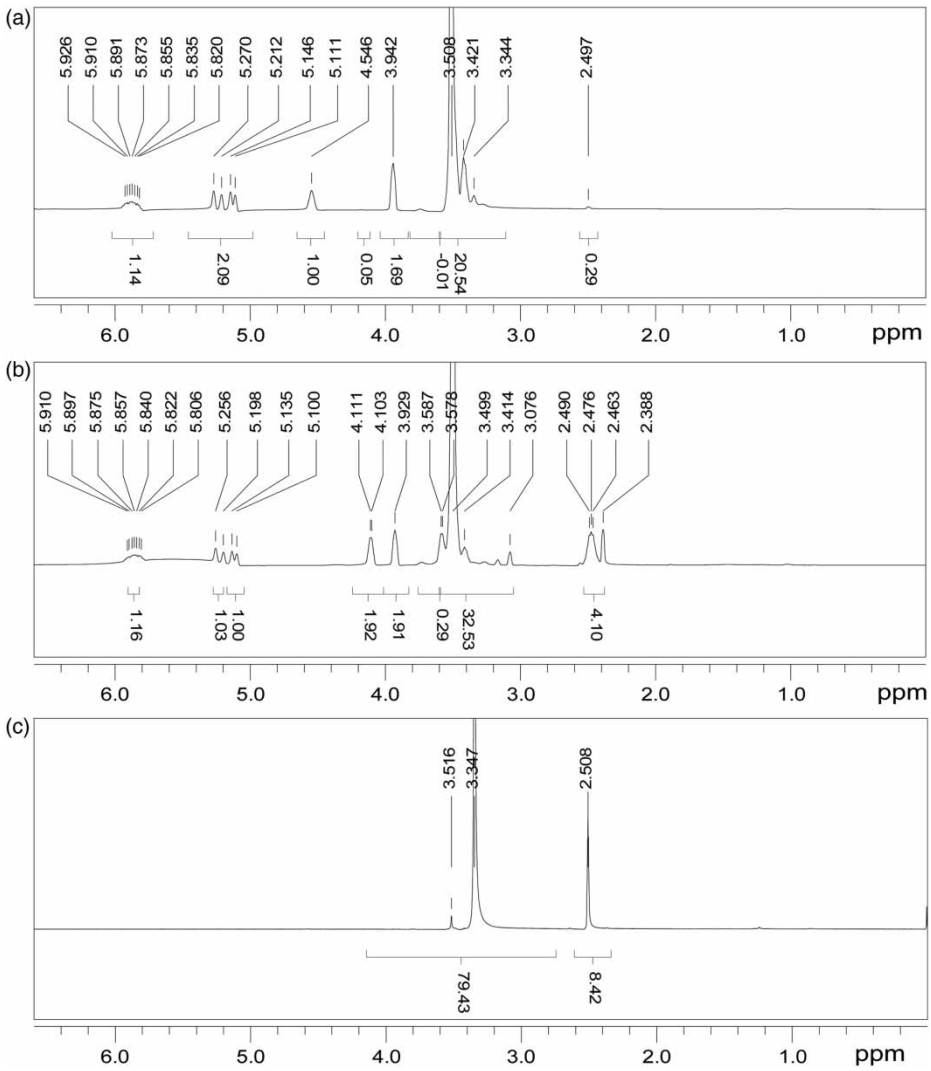

Figure 3 | ^{1}H-NMR spectra of (a) APEG, (b) APEL and (c) AA–APEL.

AA–APEL ($(CD_3)_2SO$, δppm): 2.50 (solvent residual peak of $(CD_3)_2SO$), 3.00–3.80 ($-OCH_2CH_2-$, ether groups) (Figure 3(c)). The δ3.80–6.00 ppm in (b) double bond absorption peaks completely disappeared in (c). This reveals that free radical polymerization among APEL and AA has happened. From ^{1}H-NMR analysis, it can be concluded that synthesized AA–APEL has the anticipated structure.

Influence of AA–APEL dosage on $CaCO_3$ inhibition

The scale inhibition performance of AA–APEL in simulated scale inhibition solution at different concentrations of the inhibitor is shown in Table 1. For $CaCO_3$ inhibition, 98.6% inhibition were obtained at the concentration of 8 mg/L.

Furthermore, to understand the performance, some inhibition experiments were conducted with commercial inhibitors under identical conditions. Compared to commercial inhibitors, AA–APEL had a superior ability to inhibit the $CaCO_3$ scale, with 88.5% inhibition at a level of 6 mg/L, whereas it was 65.9% for PESA at the same dosage (the best inhibitor among them). So when compared to these nonphosphorus inhibitors, $CaCO_3$ inhibition of AA–APEL is much better than that of PESA, T-225, HPMA, PAA at the same dosage. It can be shown that the order of preventing precipitation in the flask tests was AA–APEL > PESA > T-225 > PAA ≈ HPMA.

We found that PAA and HPMA contain carboxyl groups and possess molecular structures similar to AA–APEL inhibitor but can hardly control $CaCO_3$ scale even at a high dosage. It may be that the side-chain polyethylene (PEG) segments of APEL and carboxyl groups of AA might play an important role during the control of calcium carbonate scales. Taking Table 1 into account, it can be concluded that the studied copolymer AA–APEL not only solves the water eutrophication problems caused by phosphorus but also has significant inhibition efficiency in cooling water systems.

Influence of solution property on $CaCO_3$ inhibition

Solution properties have a great influence on the precipitation of calcium carbonate. In order to optimize the parameters of the recycling water process on an industrial scale, we investigated the effect of solution parameters on calcium carbonate inhibition by AA–APEL. The results are shown in Figure 4.

Figure 4(a) indicates AA–APEL provides unexceptionable calcium carbonate inhibition under conditions of water with a much higher hardness (HCO_3^- concentration kept constant and at 732 mg/L level). As illustrated in Figure 4(b), calcium carbonate inhibitory power drops 24.1% with increasing the solution pH from 7 to 12. The reason is probably that the solubility of calcium carbonate decreases when increasing the pH. At pH 8.0–9.5, the usual pH values of industry recycling water, AA–APEL still shows superior calcium carbonate inhibition. Thus, the incorporation of the high performance scale inhibitor AA–APEL into recycling water ensures a better overall system performance.

Characterization of calcium carbonate scale

The scanning electron microscope (SEM) images for collected $CaCO_3$ particles with and without inhibitors are shown in Figure 5. Compared with the two images, both

Table 1 | Comparison of $CaCO_3$ inhibition (%)

	Dosage (mg/L)							
Scale inhibitors	**2**	**4**	**6**	**8**	**10**	**12**	**14**	**16**
AA–APEL	17.8	52.6	88.5	98.6	98.3	99.1	98.9	97.9
T-225	17.6	38.2	51.2	62.3	73.1	78.8	80.7	80.1
HPMA	11.1	13.9	33.6	49.5	60.2	65.7	68.3	67.8
PAA	15.0	33.5	45.2	57.6	61.9	67.1	70.6	69.5
PESA	16.7	26.8	65.9	75.1	78.6	81.2	85.1	84.8

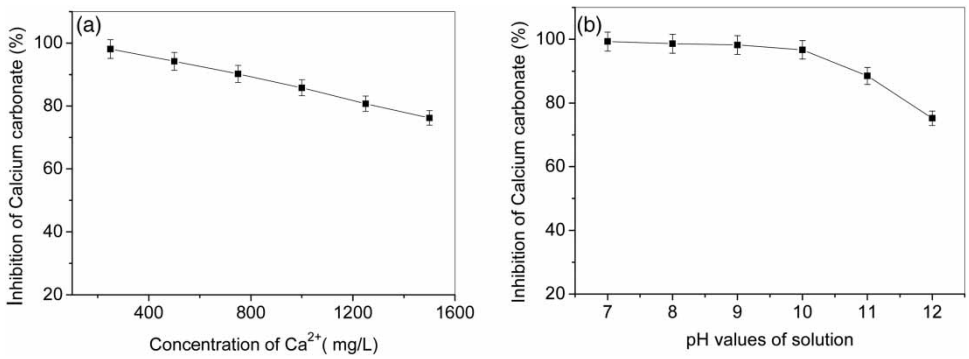

Figure 4 | Inhibition at a level of 8 mg/L AA–APEL as a function of (a) solution Ca^{2+} concentration and (b) pH.

the size and shape of the calcium carbonate precipitation were different due to the addition of the AA–APEL copolymer. Without the inhibitor, the $CaCO_3$ crystals had a regular rhombohedron shape with average particle size of about 10–40 μm. They also had a glossy surface and compact structure. This indicated that the $CaCO_3$ crystals without scale inhibitor were mainly composed of calcite, which is the most thermodynamically stable form of $CaCO_3$ crystal. In contrast, when the scale inhibitor was added into the sample, the $CaCO_3$ crystals lost their sharp edges, and the morphology was modified from rhombohedron forms to an irregular spherical with relatively loose accumulation. The irregular spherical $CaCO_3$ particle diameters were 0.5–2 μm.

The major components of the scale inhibitor were PAA and PEG. During $CaCO_3$ crystal growth, the PAA and PEG groups could affect the scale inhibition efficiency by occupying the active sites on the surface of the $CaCO_3$ crystals and changing the extent of chemical bonding with the surface.

In addition, the PEG group and −COO− group had a high chelating ability toward calcium ions to form stable chelation compounds. These would interfere with the nucleation and growth of $CaCO_3$ crystals so that the crystals became irregular. The distortion in the $CaCO_3$ crystals increased their internal stress, which would lead to crystal fractures and inhibition of the deposition of microcrystals. Previous studies suggested that vaterite could be more thermodynamically stable than calcite at certain temperatures or in the presence of some inhibitors (Kralj *et al.* 1997). Thus it was illustrated that the vaterite possessed higher thermodynamic stability than calcite in the presence of the scale inhibitor. Because vaterite has a higher solubility product and free energy than calcite, the scale was easy to dissolve and can be washed away by water.

In order to further investigate calcium carbonate crystals, the XRD was measured (Figure 6). In the absence of a copolymer, only sharp calcite reflections appeared, which coincides with the structure of the calcite crystal standard substance (Figure 6(a)). This suggested that the morphology of calcium carbonate was mainly a component of calcite. However, when the novel copolymer inhibitor

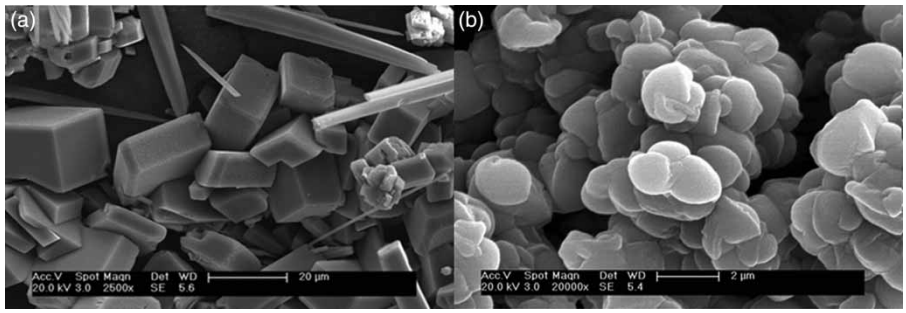

Figure 5 | SEM images of the $CaCO_3$ crystals formed (a) in the absence of AA–APEL and (b) in the presence of AA–APEL.

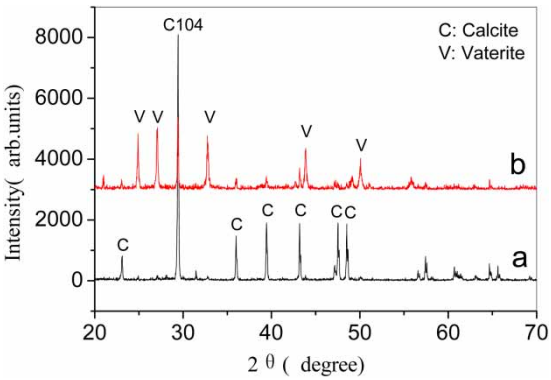

Figure 6 | XRD image of the $CaCO_3$ crystal formed (a) in the absence of AA–APEL and (b) in the presence of 5 mg/L AA–APEL.

was added (Figure 6(b)), both the intense peaks of calcite and vaterite were discovered by comparison of literature data with their XRD. In a typical aqueous system, vaterite is the first phase of calcium carbonate which then changes to a more stable phase (aragonite or calcite) over time (Greenlee *et al.* 2010). Therefore, the polymer not only can chelate with Ca^{2+}, but can also modify the formation of $CaCO_3$, which illustrates that the studies of XRD gave results consistent with SEM.

The TGA curves for $CaCO_3$ formation in the solution in the absence and presence of the polymer are shown in Figure 7. A comparison between the weight losses of the two kinds of calcium carbonate provided several new and important findings. Apparently, in Figure 7(a), the onset of scale degradation was governed by the decomposition of

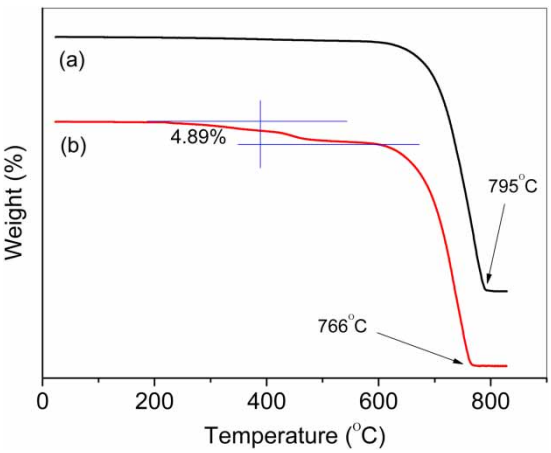

Figure 7 | TGA image of the $CaCO_3$ crystal formed in the absence of AA–APEL and in the presence of 15 mg/L AA–APEL.

$CaCO_3$ at a temperature of 647 °C. However, the scale formed in the solution adding inhibitors presented two distinct stages of mass loss. The first peak at 228 °C can be assigned to thermal decomposition of AA–APEL on the sample surface (Song *et al.* 2010), while the second peaks at 632 °C can be assigned to the degradation of $CaCO_3$ particles. Beyond expectation, $CaCO_3$ decomposed completely at 766 °C (Figure 7(b)), which was lower than the classic temperature of 795 °C (Aubert *et al.* 2006). This phenomenon is probably related to the polymer embedded in the crystal, making the crystal lattice distorted.

These three kinds of characterization of calcium carbonate scale described in Figures 5–7 indicate that the inhibitor did perform well in reducing the calcium carbonate particles. On the one hand, reduced carbonate scale formation was associated with the chelating of Ca^{2+} ions, which was attributed to the incorporation of PAA and PEG in the copolymer. On the other hand, the inhibitor was absorbed even embedded in the crystal to modify crystal structure and prevent the formation of dense, well-shaped, strongly adherent particles.

AA–APEL is a structurally well-defined diblock copolymer, depicted in Figure 8(a); the main chains are composed of allyl-terminated AA, denoted as PAA, and the side chains are made of carboxylate-capped

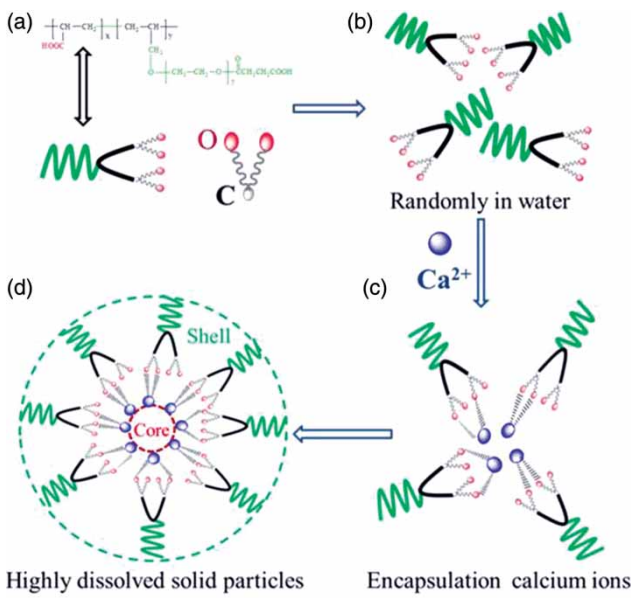

Figure 8 | Encapsulation route of calcium ions via carboxyl groups.

polyethylene glycol (PEG) segments. Both PAA and PEG segments are hydrophilic blocks and exist randomly in water (Figure 8(b)). When calcium ions are added into AA–APEL solutions, carboxyl groups in AA–APEL matrixes can recognize and encapsulate or react with positively charged calcium ions either in solutions or on the surface of inorganic minerals, such as $CaCO_3$ (Harada & Kataoka 1999; Yu *et al.* 2003). Encapsulation or interaction, between calcium ions and carboxyl groups, leads to the spontaneous formation of AA–APEL–Ca complexes (Figure 8(c)). On the other hand, when negatively charged CO_3^{2-} ions are added into solutions, the positively charged calcium ions also interact with these negatively charged ions thereby forming $CaCO_3$ crystal embryos. As a result, calcium ions acting as ties simultaneously link AA–APEL through carboxyl groups and CO_3^{2-} ions through an electrostatic attractive force. At the same time, water-compatible PEG segments, that is to say, long side chains of AA–APEL, surrounding the surfaces of crystal embryos are stable toward the aqueous phase because of their high hydrophilic properties (Figure 8(d)). Thus, $CaCO_3$ embryos incorporate into the polymer matrix of AA–APEL, and they are coated with double layers of PAA (inner layer) and PEG (outer layer). As a consequence, the aggregation of $CaCO_3$ solid particles is blocked. In addition, the long PEG side chains in the AA–APEL matrix result in steric and electrostatic repulsion. Therefore, the existing minerals do not precipitate in the presence of AA–APEL through its excellent ability to disperse solid particles.

CONCLUSIONS

A green calcium carbonate scale inhibitor AA–APEL was successfully synthesized by free polymerization of AA and APEL. ^{1}H NMR identified that AA–APEL has the expected structures. The dosage of AA–APEL copolymer has a strong effect on the formation of calcium carbonate precipitation. It can be concluded that the order of preventing the precipitation was AA–APEL > PESA > T-225 > PAA ≈ HPMA.

AA–APEL provides unexceptionable calcium carbonate inhibition under conditions of water with a much higher hardness. At the usual pH values of industry recycling water, AA–APEL shows superior calcium carbonate inhibition.

SEM images indicated that AA–APEL changes highly the morphology and size of calcium carbonate crystals during the inhibition process. XRD images indicated that AA–APEL could not only greatly inhibit the crystal growth of calcite but also transform a large amount of calcite phase to the vaterite phase.

Evaluation of the thermal stability of the $CaCO_3$ scale particles produced in the solution in the absence and presence of AA–APEL copolymer suggest that the copolymer existed in the calcium carbonate crystals. The copolymer embedded in the crystal to modify the crystal structure and prevent the formation of dense, well-shaped, strongly adherent particles.

ACKNOWLEDGEMENTS

The National Natural Science Foundation of China (No. 51077013), China Postdoctoral Science Foundation (No. 2014M560381), Jiangsu Planned Projects for Postdoctoral Research Funds (No. 1401033B), the Project of the Young Scientist Foundation of Nanjing Xiaozhuang University (No. 2013NXY89). The Municipal Key Subjects of Environmental Science and Engineering, Nanjing Xiaozhuang University, Nanjing. University Student Technology Innovation Project of Jiangsu Province (No. 201611460008Z). University Student Technology Innovation Project of Jiangsu Province (School-enterprise cooperation) (No. 201611460085H).

REFERENCES

Al Nasser, W. N., Al-Salhi, F. H., Hounslow, M. J. & Salman, A. D. 2011 Inline monitoring the effect of chemical inhibitor on the calcium carbonate precipitation and agglomeration. *Chem. Eng. Res. Des.* **89**, 500–511.

Al-Hamzah, A. A. & Fellows, C. M. 2015 A comparative study of novel scale inhibitors with commercial scale inhibitors used in seawater desalination. *Desalination* **359**, 22–25.

Alimi, F., Tlili, M., Gabrielli, C., Georges, M. & Ben Amor, M. 2006 Effect of a magnetic water treatment on homogeneous and heterogeneous precipitation of calcium carbonate. *Water Res.* **40**, 1941–1950.

Aubert, J. E., Husson, B. & Sarramone, N. 2006 Utilization of municipal solid waste incineration (MSWI) fly ash in blended cement. Part 1: processing and characterization of MSWI fly ash. *J. Hazard. Mater.* **136**, 624–631.

Fu, C., Zhou, Y., Liu, G., Huang, J., Sun, W. & Wu, W. 2011 Inhibition of $Ca_3(PO_4)_2$, $CaCO_3$, and $CaSO_4$ precipitation for industrial recycling water. *Ind. Eng. Chem. Res.* **50**, 10393–10399.

Greenlee, L. F., Testa, F., Lawler, D. F., Freeman, B. D. & Moulin, P. 2010 The effect of antiscalant addition on calcium carbonate precipitation for a simplified synthetic brackish water reverse osmosis concentrate. *Water Res.* **44**, 2957–2969.

Harada, A. & Kataoka, K. 1999 On–off control of enzymatic activity synchronizing with reversible formation of supramolecular assembly from enzyme and charged block copolymers. *J. Am. Chem. Soc.* **121**, 9241–9242.

Hasson, D., Shemer, H. & Sher, A. 2011 State of the art of friendly 'green' scale control inhibitors: a review article. *Ind. Eng. Chem. Res.* **50**, 7601–7607.

Koelmans, A. A., Van der Heijde, A., Knijff, L. M. & Aalderink, R. H. 2001 Integrated modeling of eutrophication and organic contaminant fate & effects in aquatic ecosystems: a review. *Water. Res.* **35**, 3517–3536.

Kralj, D., Brečević, L. & Kontrec, J. 1997 Vaterite growth and dissolution in aqueous solution III. Kinetics of transformation. *J. Cryst. Growth.* **177**, 248–257.

Ling, L., Zhou, Y. M., Huang, J. Y., Yao, Q. Z., Liu, G. Q., Zhang, P. X., Sun, W. & Wu, W. D. 2012 Carboxylate-terminated double-hydrophilic block copolymer as an effective and environmental inhibitor in cooling water systems. *Desalination* **304**, 33–40.

Liu, Y., Zou, C., Li, C., Lin, L. & Chen, W. 2016 Evaluation of β-cyclodextrin-polyethylene glycol as green scale inhibitors for produced-water in shale gas well. *Desalination* **377**, 28–33.

Song, L. X., Du, F. Y., Guo, X. Q. & Pan, S. Z. 2010 Formation, characterization, and thermal degradation behavior of a novel tricomponent aggregate of β-cyclodextrin, ferrocene, and polypropylene glycol. *J. Phys. Chem. B.* **114**, 1738–1744.

Wang, C., Zhu, D. Y. & Wang, X. K. 2010 Low-phosphorus maleic acid and sodium p-styrenesulfonate copolymer as calcium carbonate scale inhibitor. *J. Appl. Polym. Sci.* **115**, 2149–2155.

Wang, H. C., Zhou, Y. M., Yao, Q. Z., Ma, S. S., Wu, W. D. & Sun, W. 2014 Synthesis of fluorescent-tagged scale inhibitor and evaluation of its calcium carbonate precipitation performance. *Desalination* **340**, 1–10.

Wang, L. C., Cui, K., Wang, L. B., Li, H. X., Li, S. F., Zhang, Q. L. & Liu, H. B. 2016 The effect of ethylene oxide groups in alkyl ethoxy carboxylates on its scale inhibition performance. *Desalination* **379**, 75–84.

Yu, S. H., Cölfen, H. & Antonietti, M. 2003 Polymer-controlled morphosynthesis and mineralization of metal carbonate superstructures. *J. Phys. Chem. B* **107**, 7396–7405.

Zhang, H., Luo, X., Lin, X., Tang, P., Lu, X., Yang, M. & Tang, Y. 2016 Biodegradable carboxymethyl inulin as a scale inhibitor for calcite crystal growth: molecular level understanding. *Desalination* **381**, 1–7.

First received 16 August 2016; accepted in revised form 31 January 2017. Available online 15 February 2017